

平成 28 年度  
三重大学大学院 生物資源学研究科  
修士論文

**The role of the existence of the Okhotsk Sea in the weakening  
of the northern hemisphere zonal mean flow in winter**

—オホーツク海の存在が弱める冬季北半球規模帯状平均流—

*Weather and Climate Dynamics Division  
Graduate school of Bioresources  
Mie University*

515M203

Kenta Kawasaki

*Supervisor:* Prof. Yoshihiro Tachibana

February 13, 2017

## ABSTRACT

It is commonly known that the development of Arctic Oscillation (AO) is one of the most famous climatic phenomenon in winter season. Some studies pointed out that the atmospheric response of the changed troposphere and stratosphere by thermal response caused by the fluctuation of Arctic sea-ice affects extremely to winter AO. However, little has been known that whether or not the marginal sea in mid-latitude affects to the atmospheric circulation in winter season. The Okhotsk Sea, which is located to the north of Japan, has characteristic that be warmer extremely than surrounding continental in winter season. The variability of sea-ice areas in the Okhotsk Sea was shown that impacted to the strength of Aleutian low in winter by propagated of the stationary Rossby wave caused by the different of thermal response. Therefore, the Okhotsk Sea has the potential that impact to the large-scale atmospheric circulation and it is also important climatologically that understand its mechanism. This study focused on the role of existence of the Okhotsk Sea for the large-scale atmospheric circulation in winter by using Atmospheric General Circulation Models (AGCM). One GCM is executed without the Okhotsk Sea, in which was changed to continent as if the Okhotsk Sea was totally landfilled (LAND). The other (CTL) is a under the boundary condition of climatic seasonal changes of the Sea Surface Temperature (SST) over the globe. The comparison of the CTL with the LAND showed that the cold air (hot air) is strengthened in the Europe (eastern

Siberia) in December by the strengthened advectations in the each areas by the dominated wave train caused by the existence of the Okhotsk Sea. Eliassen-Palm flux (EP-flux) shown the propagation of planetary wave is propagated upward and converged in stratosphere by forced the poleward eddy heat transport caused by strengthened the temperature and meridional wind associated with wave train. Troposphere and stratosphere were coupled from December to January because stratosphere at high latitude was warmed by the decelerated westerly wind that associated with convergence of EP-flux. Moreover, in January, EP-flux propagated downward and converged at troposphere. Therefore, the Polar high is forced at troposphere by the decelerated westerly jet stream caused by the convergence of EP-flux. The strengthened Polar high warms the Arctic and cools the northern Eurasian and American continent. In consequence, the Okhotsk Sea plays a significant role in the strengthening the Polar high and its associated the variability of temperature at northern hemisphere in winter season.

# **Contents**

<b>1. Introduction .....</b>	<b>5</b>
<b>2. Data and Indices .....</b>	<b>7</b>
<b>2.1 Model and Simulations .....</b>	<b>7</b>
<b>3. Results .....</b>	<b>9</b>
<b>4. Discussion and conclusion .....</b>	<b>12</b>
<b>Acknowledgements.....</b>	<b>14</b>
<b>Reference.....</b>	<b>15</b>
<b>List of Figures.....</b>	<b>17</b>

## 1. Introduction

The Okhotsk Sea plays an important role in the climate of the surrounding areas; Japan, Russian Far East, and the Pacific Ocean. Many of the Kuril Islands, located between the Okhotsk Sea and the Pacific Ocean, are uninhabited. The Cold Okhotsk Sea might make these islands uninhabitable in spite of rich fishery resource there. In fact, summertime Sea surface Temperature (SST) as low as 5°C in Okhotsk Sea cold spots [e.g., Tachibana et al., 2008; Tokinaga and Xie, 2009; Nishikawa et al., 2014]. These cold SSTs are lower than any reported summertime SSTs in other Northern Hemisphere seas at the same latitude. Nakamura and Fukamachi 2004 and Tachibana et al 2004 showed that the air temperature contrast between the Okhotsk Sea and a surrounding continent plays a role in the formation of the Okhotsk high. The Okhotsk high is accompanied with cold fog [e.g., Tachibana et al., 2008], and the cold SST with fog strengthens the Okhotsk high [Tokinaga and Xie, 2009; Nishikawa et al., 2014]. Also, the Okhotsk Sea further has an impact on remote climate, not only such a surrounding area like Kuril Islands. For example, the Okhotsk sea-ice has an influence on the strength of North Atlantic Oscillation [Yamamoto et al., 2005]. Furthermore, [Honda et al., 1999] reported that the variability of sea-ice areas in the Okhotsk Sea impacts on the strength of winter Aleutian low by propagated of the stationary Rossby wave caused by the different of thermal response. These studies suggestively provide us with the potential importance of the existence of the Okhotsk Sea for the climate locally and remotely. Because actual climate in an area is

the result from complex interaction with many climatic subsystems, the roles of the Okhotsk Sea and other subsystems in the local and remote climate are undistinguishable. Therefore, to distinguish the role of the Okhotsk Sea, following thought experiment is useful. Without the Okhotsk Sea, i.e., if the Okhotsk Sea were land, how would atmospheric circulation patterns be locally and remotely? An ideal atmospheric general circulation model (AGCM) experiment is an excellent tool to answer this question. Numerical model is able to the land as a lower boundary condition. Comparison between the AGCM experiment with and without the Okhotsk Sea is able to isolate the importance of the existence of the Okhotsk Sea. The purpose of the present study is to understand the role of the Okhotsk Sea by executing abovementioned two AGCMs with targeting the winter climate. It should be noted that the AGCM without the Okhotsk Sea does not aim to simulate climate of the past but only to utilize to understand the role of the Okhotsk Sea in the present climate deeply.

## **2. Data and Indices**

### **2.1 Model and Simulations**

We used the AGCM for Earth Simulator (AFES) [Ohfuchi et al., 2004, 2007; Enomoto et al., 2008; Kuwano-Yoshida et al., 2010] version 4.1. The horizontal wavenumber is 79 (T79; approximately 1.5° horizontal resolution), and the vertical levels are 56 (model top is about 60km). We used the merged Hadley-National Oceanic and Atmospheric Administration (NOAA)/Optimum Interpolation (OI) Sea Surface Temperature (SST) and Sea-Ice Concentration (SIC) [Hurrell et al., 2008] datasets. This model does not use SIC directly. This model used the Sea Ice Thickness (SIT) from converted the SIC. The SIT condition and other conditions were performed under the same conditions as the Nakamura et al., 2015. The initial condition used the January 1979 monthly mean from the Japanese 25-year Reanalysis (JRA-25)/Japan Meteorological Agency (JMA) Climate Data Assimilation System (JCDAS) reanalysis data [Onogi et al., 2007]. The sea run is a control run (CTL) under the boundary condition of monthly changes of the 5-year averaged SST and SIT for the period of 1979-1983. The land run (LAND) used the same boundary condition as CTL but ground condition was changed to an eastern part of the Eurasian continent as if the Okhotsk Sea was totally landfilled (Fig.1). A height of ground in Okhotsk area was same height as sea surface (about 0m). The ground condition in Okhotsk area was same as Siberia and Japan. We carried out 30-year integrations after 2-year spin-up and examined the differences between the 30-year averages of CTL and LAND (CTL

minus LAND).



### 3. Results

Figure 2a shows anomalies of net heat flux between CTL and LAND (CTL minus LAND) in January. Strong positive anomalies are found in the Okhotsk Sea. This result shows that the Okhotsk Sea has a function of hot source in winter season, because the difference of heat capacity between Sea and LAND. Figure 2b shows anomalies of temperature at 2m. Positive anomalies centered on the Okhotsk Sea are caused by heat transports from sea to atmosphere. The CTL forms surface temperature fields of about 8°C warmer than the LAND. Next, we examine to impact of warm surface temperature over the Okhotsk Sea to pressure fields. Figure 3a shows anomalies of Sea Level Pressure (SLP). Negative anomalies in the Okhotsk Sea are caused by strengthened upward flow by strong warm temperature. Characteristic positive anomalies are found in the Arctic area. This Arctic high is barotropic to middle troposphere (Fig. 3b). Because the Arctic high strengthened the cold advection, the Siberia and Canada become cold (Fig. 4a and 4b). The warm temperature anomalies over the Arctic area are caused by activated the downward flow by the strengthened the Arctic high. These results imply that the existence of the Okhotsk Sea strengthen the Arctic high such as the AO minus.

Next, we examined to reason of strengthened the Arctic high by the existence of Okhotsk Sea. Figure 5 shows anomalies of zonal wind at 300hPa. Positive anomalies are found in the middle latitude. Strong negative anomalies are found in the high latitude. Weakening of the westerly jet stream at high latitude imply that strengthen the anticyclone in the Arctic area relatively. Figure 6

shows seasonal evolution of anomalies of zonal cross section of 50°N - 60°N averaged zonal wind. The westerly jet stream decelerated in late December over the stratosphere. This decelerated jet stream are continued in January troposphere. Figure 7 shows anomalies of Eliassen-Palm flux (EP-flux) [Andrews, 1983] and divergence of EP-flux. Anomalies of convergence of EP-flux are found at middle troposphere and divergence of EP-flux are found at stratosphere. Anomalies of EP-flux are propagated downward to respond to this results. Because the convergence of EP-flux weaken the westerly jet stream, the Arctic high was strengthened by decelerated jet stream caused by the convergence of EP-flux at middle troposphere. These results indicates that the reason of strengthen the Arctic high is caused by the effect of atmosphere in late December. Figure 8 shows anomalies of EP-flux and divergence of EP-flux in late December. Anomalies of divergence of EP-flux are found at high-latitude troposphere. Anomalies of EP-flux propagated upward from this divergence area to stratosphere convergence area. Because the vertical component of EP-flux is determined by the eddy heat flux, we calculated anomalies of eddy heat flux in following expression (1).

$$V'T' = V'_a T'_a + V'_a T'_a + V'_c T'_a + V'_c T'_c \quad (1)$$

where V and T are meridional wind and temperature, ' is anomalies from zonal mean fields, a is high-pass filter weighted 5days and c is low-pass filter weighted 5days. Because orders of terms that include component of day-to-day disturbance are low compared with component of low-pass filter,

we disregarded components of high-pass filter. Figure 9a shows anomalies of eddy heat flux at 100hPa. Positive anomalies of eddy heat flux are found at Aleutian, eastern Canada and Europa. Figure 9b shows anomalies of geopotential height at 100hPa. Positive anomalies are found around the Canada. Positive temperature anomalies are warmed by adiabatic compression caused by the strengthening high. Negative temperature anomalies are chilled by the activated cold advection caused by the northerly winds which associated with the strengthened Aleutian low and Siberian low. Thus, positive anomalies of eddy heat flux in Figure 9a are activated by the strengthened wave train. To examine the strengthened wave train, we calculated the wave activity flux. Figure 9c shows the anomalies of wave activity flux and geopotential height at 500hPa. Positive anomalies are found at the Okhotsk, western America and northern Canada. Negative anomalies are found at the Aleutian, Atlantic and Siberia. Anomalies of wave activity flux propagated from the strengthened Aleutian low to global. Therefore, this strengthened wave train are formed by the propagated wave activity flux caused by the strengthened Aleutian low. The strengthened Aleutian low is formed by the thermal response caused by the existence of the Okhotsk Sea. This response is same as the [Honda et al., 1999]. Therefore, these results imply, which are caused by the effect of the hot source by the existence of Okhotsk Sea.

#### **4. Discussion and Conclusion**

We performed a numerical experiments using an AGCM under the two conditions: one GCM is the Okhotsk Sea was changed to continental (LAND run) and the other is boundary condition of climatic seasonal changes of the SST (CTL run), to examine the influence of existence of the Okhotsk Sea on the atmospheric circulation in winter season. The major difference in experiments of conditions under the SST and continental in the Okhotsk Sea area is thermal heat capacity. In late December, lower layer of atmosphere around the Okhotsk Sea is warm relatively by effect that sea is hard to warm in compared to condition of continental. The CTL works to have a capability as strong hot source in the Okhotsk Sea. Therefore, the theory of the strengthened Arctic high is achieved by discuss the following some processes caused by this effect. First, this relative hot source forces formation of significant strong positive hot temperature anomalies in directly above in the Okhotsk Sea (Fig. 2c) and the formed hot temperature anomalies are strengthening the Aleutian low, because the effect of thermal response such as [Honda et al., 1999]. This strengthened Aleutian low activated the wave activity flux and its formed the wave train at middle troposphere (Fig. 9b). The formed wave train strengthened eddy heat flux at upper layer at troposphere (Fig. 9a). Therefore, the westerly jet stream at stratosphere is weaken. This effect is continuing to January, which effect activated the EP-flux convergence to troposphere. Convergence of EP-flux weaken the westerly jet stream at middle troposphere (Fig. 5). Thus, the weakening jet stream at troposphere strengthen Arctic high. Given these facts, it suggest that the existence of current hot Okhotsk Sea has the role

for change the troposphere and stratosphere circulation and strengthen the AO minus. In conclusion, we confirmed the new mechanism of the strengthening Arctic high and the AO minus by the activated the convergence of EP-flux at troposphere caused by the effect of changed troposphere and stratosphere by the thermal response of existence of Okhotsk Sea. Moreover, we consider that if the Okhotsk Sea will be warming by the Global warming, the AO minus will be strengthened by the hot source in Okhotsk Sea.

## **Acknowledgements**

I extend grateful thanks for Prof. Yoshihiro Tachibana who is my supervisor. Prof. Tachibana taught me the amusingness to research for meteorology or climate and he gave me a chance to innovative research, irreplaceable meteorological knowledge and technics for analysis.

I extend special thanks to Dr. Koji Yamazaki for their very helpful discussions. Members of Climate and Ecosystem Dynamics Laboratory provided some advices for my research. I would to thanks for them.

## Reference

Tachibana, Y., K. Iwamoto, H. Ogawa, M. Shiohara, K. Takeuchi, and M. Wakatsuchi, 2008:

Observational study on atmospheric and oceanic boundary-layer structures accompanying the Okhotsk anticyclone under fog and non-fog conditions. *Journal of Meteorological Society of Japan*, **86**, 753-771.

Tokinaga, H., and S. -P. Xie, 2009: Ocean tidal cooling effect on summer sea fog over the Okhotsk

Sea. *J. Geophys. Res. –Atmos.*, **114**, D14102, doi: 10. 1029/2008JD011477.

Nishikawa, H., Y. Tachibana, and Y. Udagawa, 2014: Radiosonde observational evidence of the

impact of an extremely cold SST spot on a mesoscale anticyclone. *Journal of Geophysical Reserch Atmosphere*, **119**, 9183-9195.

Nakamura, H. and T. Fukamachi, 2004: Evolution and dynamics of summertime blocking over the

blocking and the associated surface Okhotsk high. *Quart. J. Roy. Meteor. Soc.*, **130**, in press.

Tachibana, Y., T. Iwamoto, and M. Ogi, 2004: Abnomal meridional temperature gradient and its

relation to the Okhotsk high. *Journal of Meteorological Society of Japan*, **82**, 1399-1315.

Honda, M., K. Yamazaki, H. Nakamura, and K. Takeuchi, 1999: Dynamic and Thermodynamic

Characteristics of Atmospheric Response to Anomalous Sea-Ice Extent in the Sea of Okhotsk. *J. Climate*, **12**, 3347-3358.

Ohfuchi, W., and Coauthors, 2004: 10-km Mesh Meso-scale Resolving Simulations of Global

Atmosphere on the Earth Simulator: Preliminary Outcomes of AFES (AGCM for the Earth

Simulator). *J. Earth Simul*, **1**, 8-34.

Hurrell et al, 2008: Merged Hadley-NOAA/OI Sea surface temperature & Sea-Ice concentration

Nakamura, T., K. Yamazaki, Iwamoto, M. Honda, Y. Miyoshi, Y. Ogawa, and J. Ukita, 2015: A

negative phase shift of the winter AO/NAO due to the recent Arctic sea-ice reduction in late

autumn. *J. Geophys. Res. Atmos.*, **120**, 3209-3227.

Andrews, D.G., 1983: A finite-amplitude Eliassen-Palm theorem in isentropic coordinates. *J. Atmos.*

*Sci.*, **40**, 1877-1883.



## List of Figures

**Figure 1** Ground parameter of CTL run and LAND run (blue: cold-deciduous forest, yellow: grassland, red: cultivation zone).

**Figure 2a** Anomalies of net heat flux [ $\text{W}/\text{m}^2$ ] between CTL and LAND (color shading). Significance levels above 95% based on t-test are hatched.

**Figure 2b** Anomalies of temperature at 2m [ $^{\circ}\text{C}$ ] between CTL and LAND (color shading). Significance levels above 95% based on t-test are hatched.

**Figure 3a** Anomalies of Sea level pressure [hPa] between CTL and LAND (color shading). Significance levels above 95% based on t-test are hatched.

**Figure 3b** Anomalies of geopotential height at 500hPa [m] between CTL and LAND (color shading). Significance levels above 95% based on t-test are hatched.

**Figure 4a** Anomalies of temperature advection at 850hPa [ $^{\circ}\text{C}/1^{\circ}\text{lat}/\text{lon}$ ] between CTL and LAND (color shading). Contours are climatology values in CTL run [K]. Vectors are anomalies of horizontal wind [m/s].

**Figure 4b** Anomalies of temperature at 2m [ $^{\circ}\text{C}$ ] between CTL and LAND (color shading). Significance levels above 95% based on t-test are hatched.

**Figure 5** Anomalies of zonal wind [m/s] between CTL and LAND (color shading). Significance levels above 95% based on t-test are hatched.

**Figure 6** Anomalies of EP-flux [ $\text{m}^2/\text{s}^2$ ] between CTL and LAND (color shading). Contours are

anomalies of divergence of EP-flux [ $\text{m}^2/\text{s}^2$ ].

**Figure 7** Anomalies of seasonal evolution of 50N-60N averaged zonal wind [ $\text{m}/\text{s}$ ] between CTL and LAND (color shading). Significance levels above 95% based on t-test are hatched.

**Figure 8** Anomalies of EP-flux [ $\text{m}^2/\text{s}^2$ ] between CTL and LAND (color shading). Contours are anomalies of divergence of EP-flux [ $\text{m}^2/\text{s}^2$ ].

**Figure 9a** Anomalies of  $t'$  [ $^{\circ}\text{C}$ ] between CTL and LAND (color shading). Contours are anomalies of  $v'$  [ $\text{m}/\text{s}$ ].

**Figure 9b** Anomalies of geopotential height at 100hPa [ $\text{m}$ ] between CTL and LAND (color shading).

**Figure 9c** Anomalies of geopotential height at 500hPa [ $\text{m}$ ] between CTL and LAND (color shading). Vectors are anomalies of wave activity flux [ $\text{m}^2/\text{s}^2$ ].

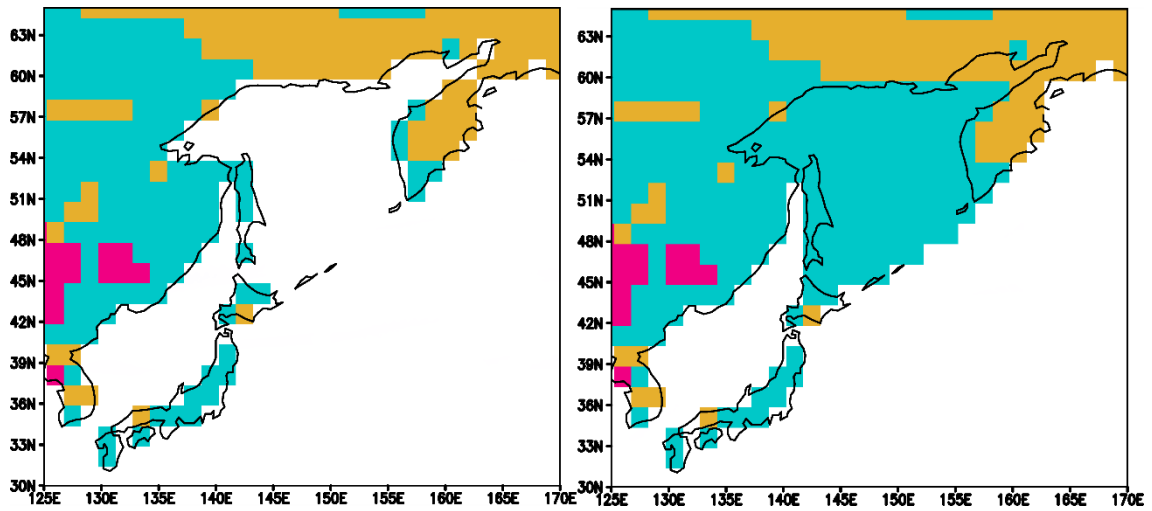


**Figure 1** Ground parameter of CTL run and LAND run (blue: cold-deciduous forest, yellow: grassland, red: cultivation zone).

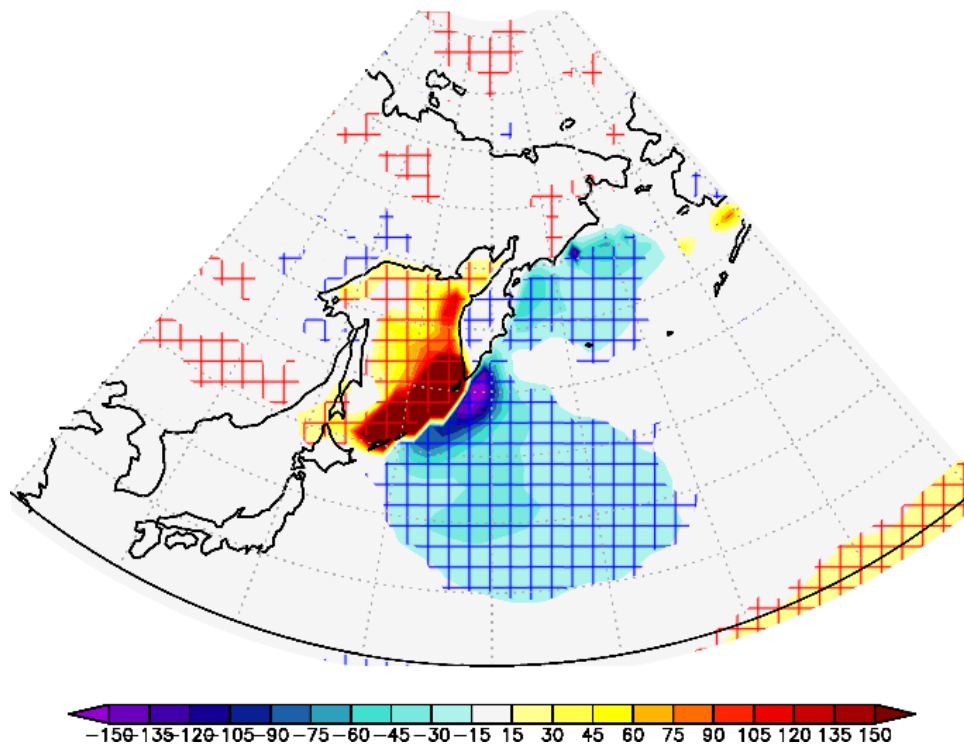


**Figure 2a** Anomalies of net heat flux [ $\text{W/m}^2$ ] between CTL and LAND (color shading). Significance levels above 95% based on t-test are hatched.

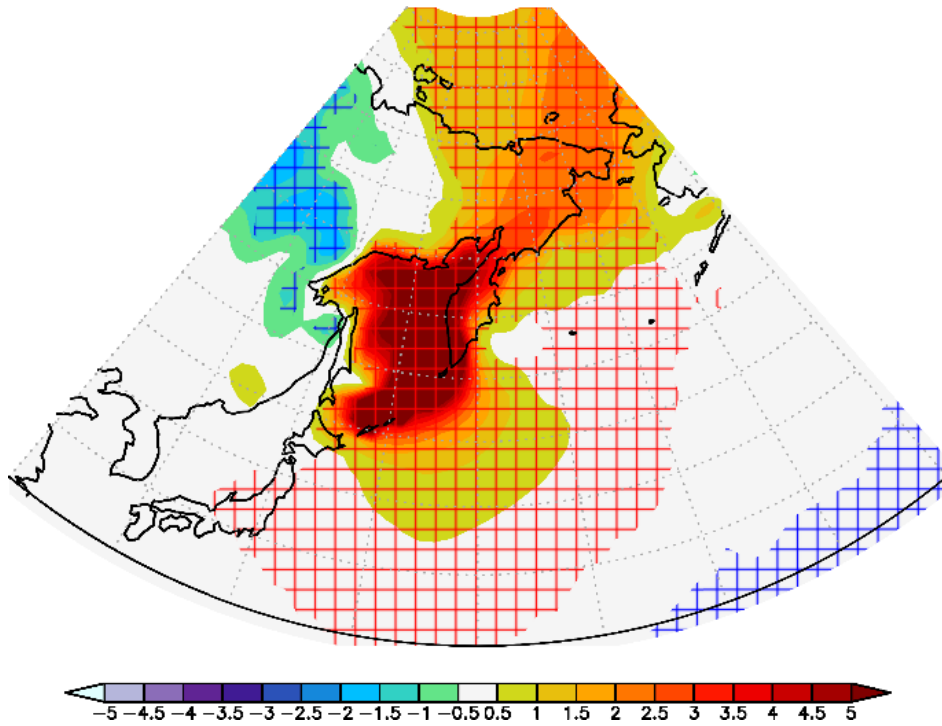


**Figure 2b** Anomalies of temperature at 2m [°C] between CTL and LAND (color shading). Significance levels above 95% based on t-test are hatched.

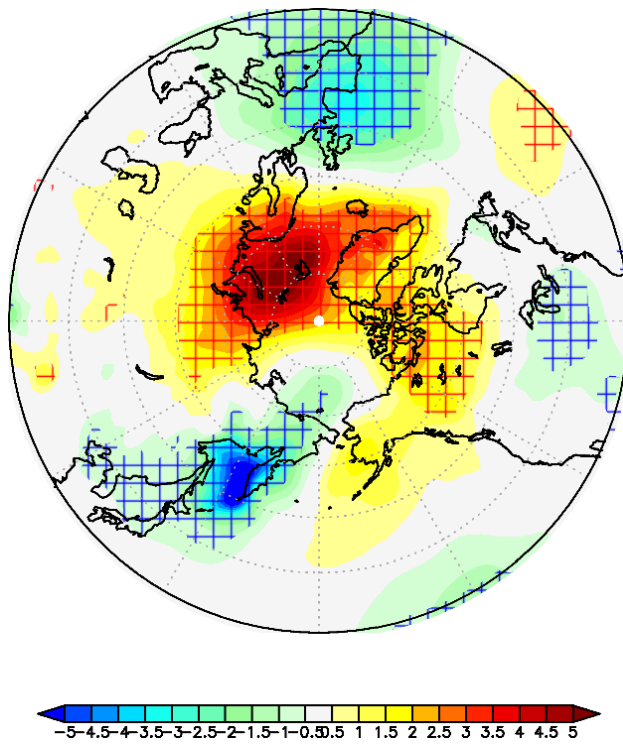


**Figure 3a** Anomalies of Sea level pressure [hPa] between CTL and LAND (color shading). Significance levels above 95% based on t-test are hatched.

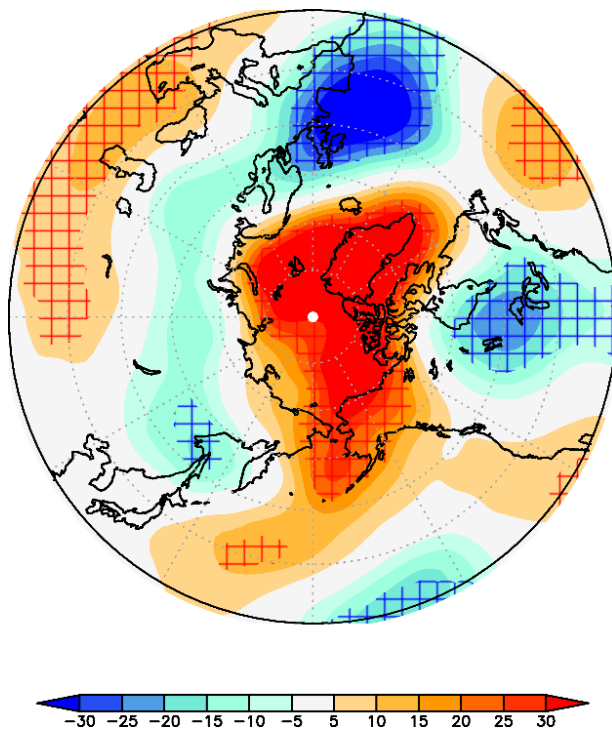


**Figure 3b** Anomalies of geopotential height at 500hPa [m] between CTL and LAND (color shading). Significance levels above 95% based on t-test are hatched.

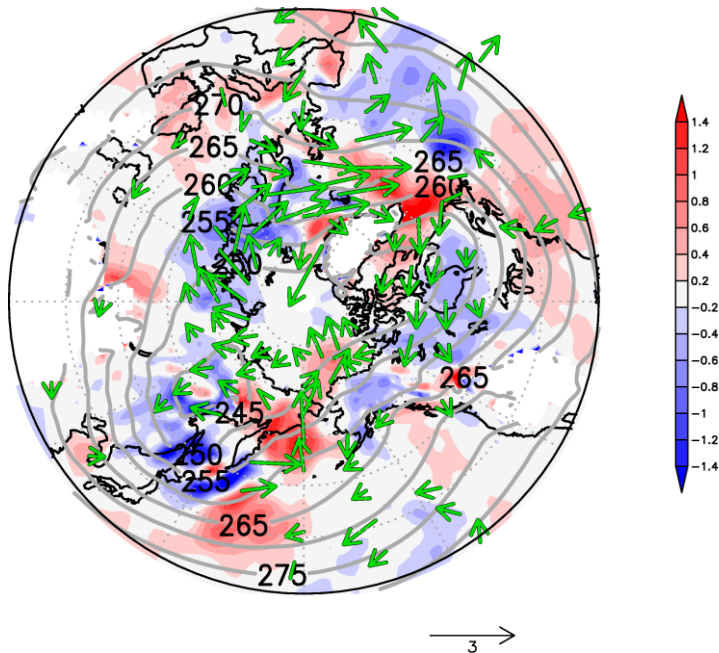


**Figure 4a** Anomalies of temperature advection at 850hPa [ $^{\circ}\text{C}/1^{\circ}\text{lat}/\text{lon}$ ] between CTL and LAND (color shading). Contours are climatology values in CTL run [K]. Vectors are anomalies of horizontal wind [m/s].

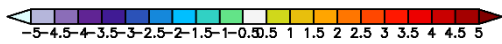
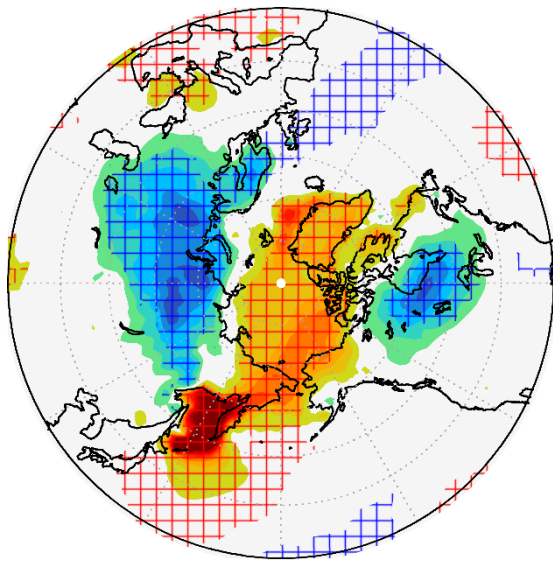


**Figure 4b** Anomalies of temperature at 2m [ $^{\circ}\text{C}$ ] between CTL and LAND (color shading). Significance levels above 95% based on t-test are hatched.

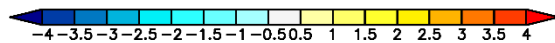
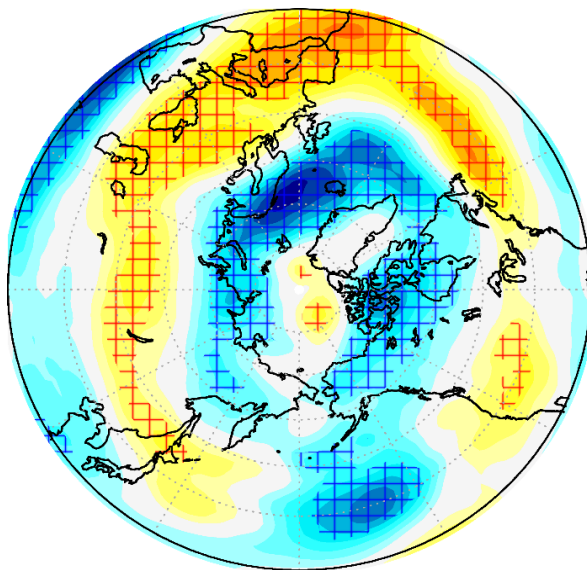


**Figure 5** Anomalies of zonal wind [m/s] between CTL and LAND (color shading). Significance levels above 95% based on t-test are hatched.

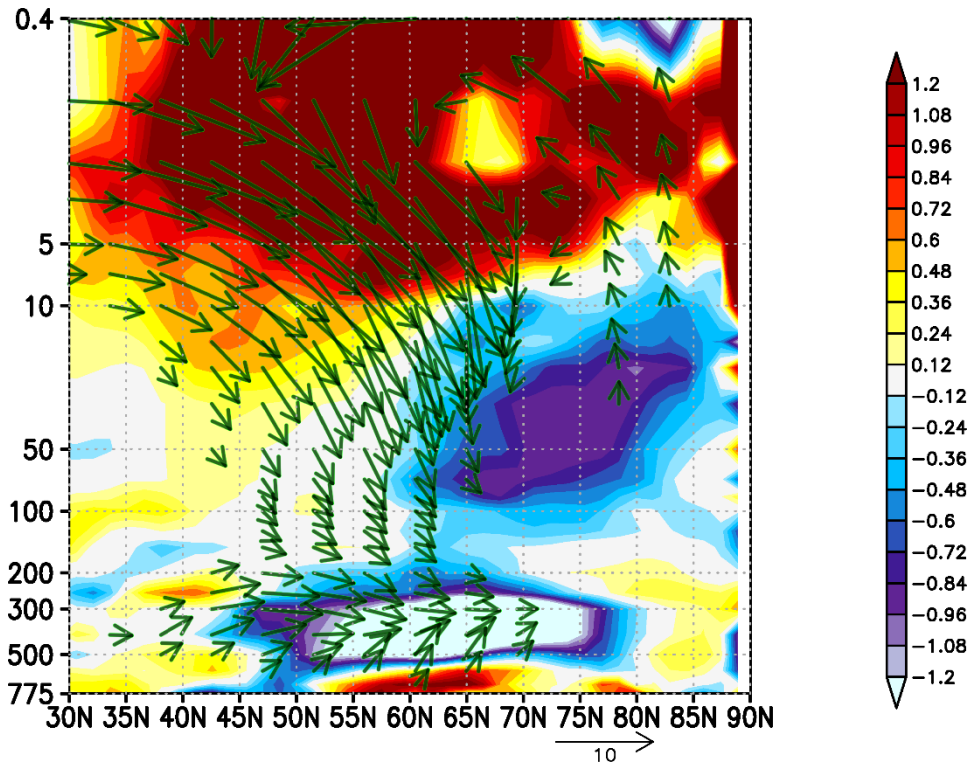


**Figure 6** Anomalies of EP-flux [ $\text{m}^2/\text{s}^2$ ] between CTL and LAND (color shading). Contours are anomalies of divergence of EP-flux [ $\text{m}^2/\text{s}^2$ ].

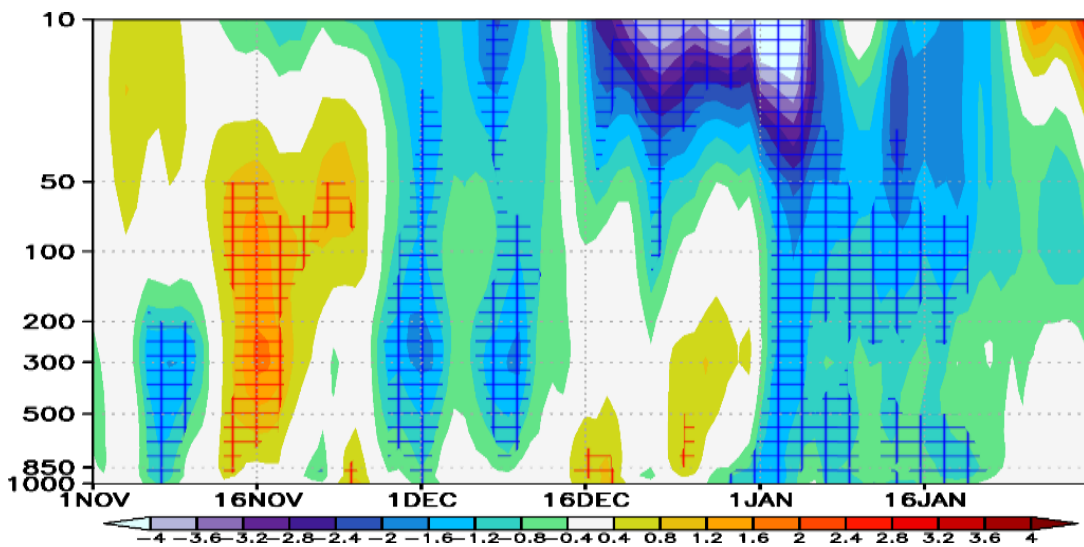


**Figure 7** Anomalies of seasonal evolution of 50N-60N averaged zonal wind [ $\text{m}/\text{s}$ ] between CTL and LAND (color shading). Significance levels above 95% based on t-test are hatched.

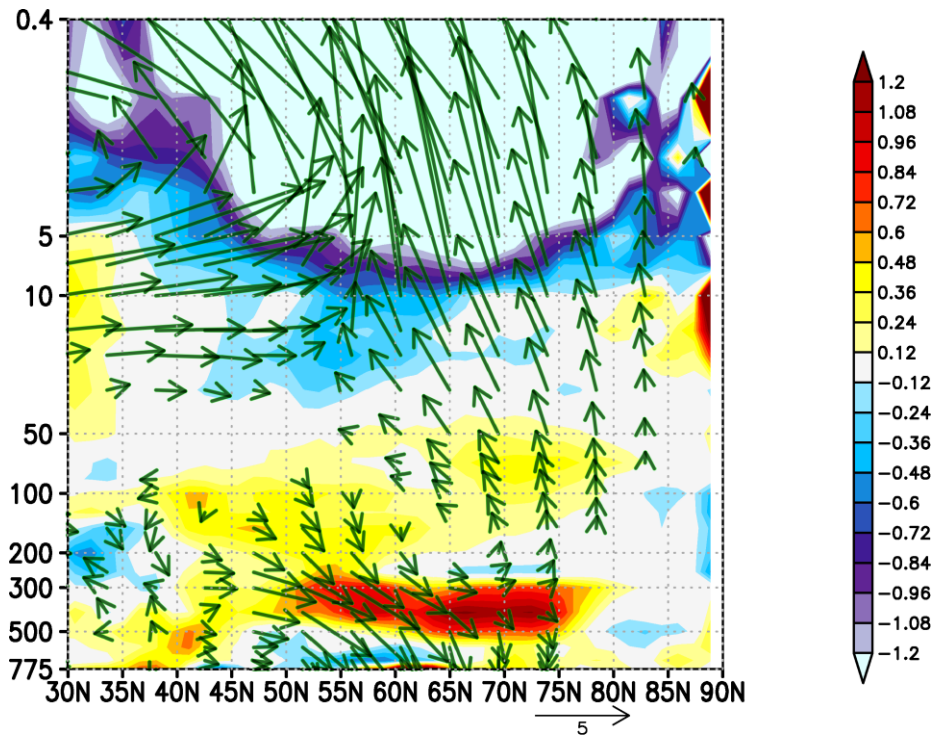


**Figure 8** Anomalies of EP-flux [m<sup>2</sup>/s<sup>2</sup>] between CTL and LAND (color shading). Contours are anomalies of divergence of EP-flux [m<sup>2</sup>/s<sup>2</sup>].

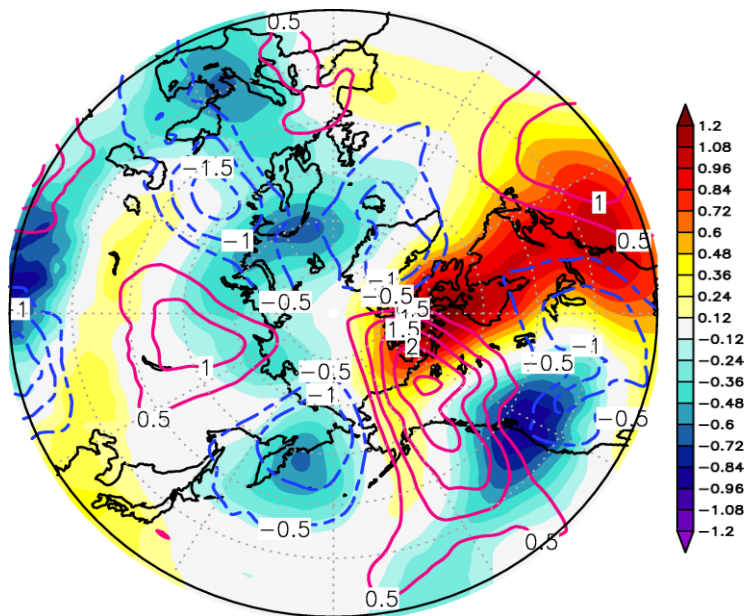


**Figure 9a** Anomalies of t' [°C] between CTL and LAND (color shading). Contours are anomalies of v' [m/s].



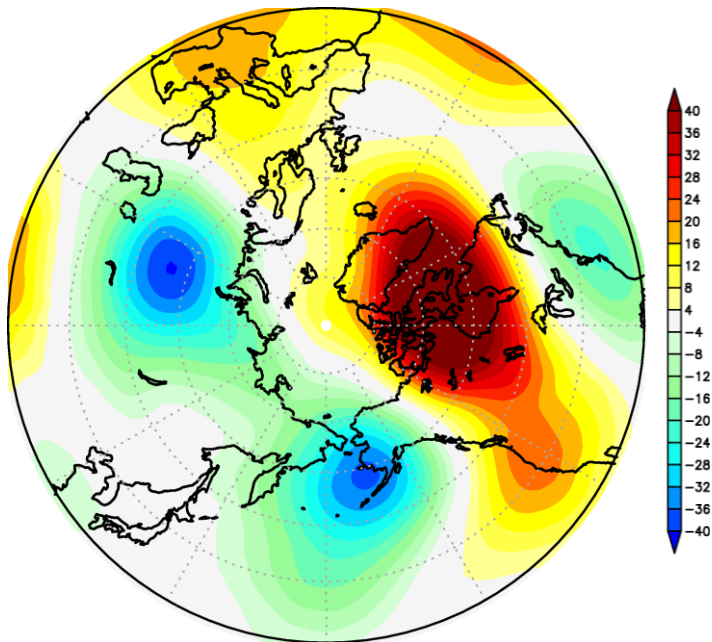


**Figure 9b** Anomalies of geopotential height at 100hPa [m] between CTL and LAND (color shading).

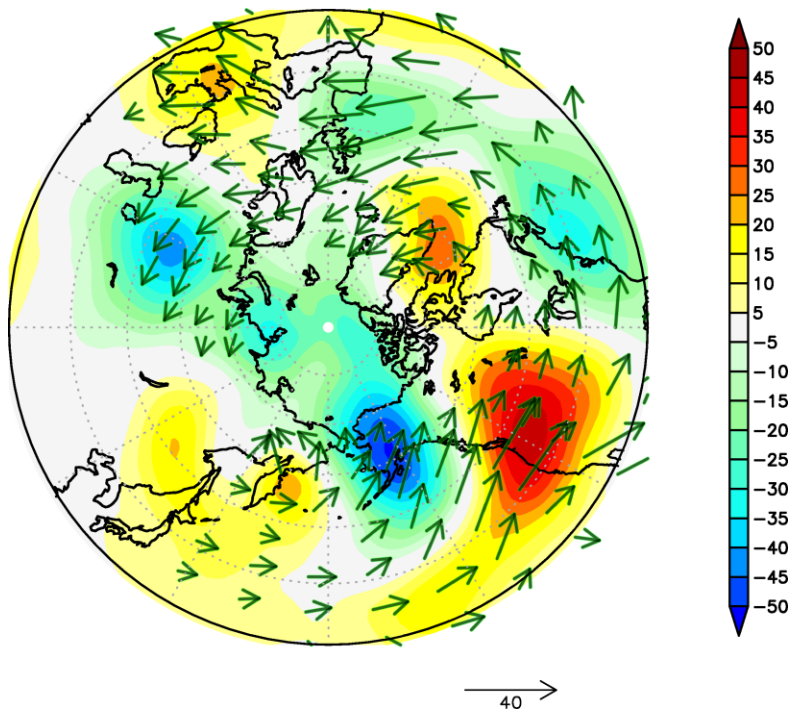


**Figure 9c** Anomalies of geopotential height at 500hPa [m] between CTL and LAND (color shading). Vectors are anomalies of wave activity flux [ $\text{m}^2/\text{s}^2$ ].